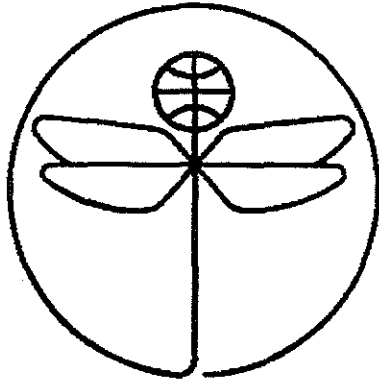


TWENTY FIRST EUROPEAN ROTORCRAFT FORUM



Paper No VII. 9

**THE EFFECTS OF BLADE FLEXIBILITY ON THE CONTROL
RESPONSE OF ARTICULATED-ROTOR HELICOPTERS IN HOVER**

BY

Bruce D. Kothmann
H.C. Curtiss, Jr.

Department of Mechanical and Aerospace Engineering
Princeton University
Princeton, New Jersey, USA

August 30 - September 1, 1995
SAINT - PETERSBURG, RUSSIA

Paper nr.: VII.9

The Effects of Blade Flexibility on the Control Response of an
Articulated-Rotor Helicopters in Hover.

B.D. Kothmann; H.C. Curtiss

TWENTY FIRST EUROPEAN ROTORCRAFT FORUM
August 30 - September 1, 1995 Saint-Petersburg, Russia

The Effects of Blade Flexibility on the Control Response of Articulated-Rotor Helicopters in Hover

Bruce D. Kothmann

H.C. Curtiss, Jr.

Department of Mechanical and Aerospace Engineering
Princeton University
Princeton, New Jersey, USA

Abstract

Relatively little research has been done to determine the effects of blade flexibility on helicopter control response in the frequency range of 0.05 to 1.0 per rev. Accurate predictions of the coupled rotor-body dynamics in this frequency range is of importance as the response bandwidth of modern helicopters continues to increase. This paper describes a novel technique for the development of analytical (non-numerical) equations for the coupled dynamics of the fuselage and the flexible rotor blades. Simplified subsets of the full equations are used to elucidate the physical mechanisms by which blade flexibility influences the response of vertical acceleration, yaw rate, and roll rate to on-axis control inputs for articulated rotor helicopters in hover. The effects are generally shown to be small, but not inconsequential, especially those effects associated with a powerful lag damper. The use of nonphysical hinge springs and/or dampers, or other variations in physical parameters of a rigid blade model, is shown to be adequate to account for some, but not all, of the observed effects.

Introduction

Blade flexibility has been the subject of considerable research in the vertical flight community over the past 40 years or more. From the perspective of flight dynamics, a convenient way to organize and review previous research efforts is to group them according to the range of frequencies in which the analyses are intended to be applicable, as shown graphically in Figure 1, where frequencies have been normalized by rotor RPM. A brief review of the significant results of each of these groups will motivate the present work.

The most basic characterization of the effects of blade flexibility on helicopter flight dynamics, valid at low frequencies (below about 0.1 per rev), may be derived using the classical quasi-static rotor

analysis. From this point of view, blade flexibility impacts the steady-state response of the rotor to control inputs and body motions and consequently changes the forces and moments transmitted to the hub. Because such analyses are quasi-steady, they do not, by definition, include coupling of the rotor dynamics to the body motion. Therefore, the rotor calculations may be performed "off-line", effectively producing a map of the rotor forces and moments which may be compared to the map for a rotor with rigid blades. The differences between the two maps are indicative of "flexibility effects" and have implications for calculation of the trim condition and the low frequency modes of the body motion. An example is the effect of torsional deflections due to a chordwise offset of blade center of mass on the stability of the low frequency body modes, as reported by Blake and Alansky [1], and more recently by Celi [2].

At high frequencies, roughly defined as those at or above the rotor speed, there is a substantial body of literature on modelling flexible blades (see the reviews by Chopra [3] and Friedmann [4]), with the finite element method being the most popular type of analysis in current use. In this frequency range, emphasis has been placed on the difficult problem of rotor stability, which has been shown to depend quite critically on the interaction of "small" aerodynamic and elastic coupling terms [5]. Prediction of harmonic bending stresses and transmission of vibrational loads to the hub have also been investigated in some detail, although substantial difficulties remain, particularly with the prediction of chordwise stresses. Because of their focus on high-frequency effects, the great majority of these investigations have emphasized shaft-fixed calculations, which are not directly applicable to the prediction of control response.

Accurate prediction of the vehicle dynamics at intermediate frequencies, in the range of 0.1 to 1.0 per rev, is of increasing importance, as technological advances, in the form of hingeless rotors and digital flight control systems, make possible dramatic decreases in the control response time. Many studies [e.g. 6, 7] have considered the now well known

Presented at the Twenty-First European Rotorcraft Forum, St. Petersburg, Russia, August 1995.

implications of coupled rotor-body dynamics, which occur in this frequency range, for the design of automatic flight control systems. However, there is a near absence of research on the specific effects of blade flexibility in this important, intermediate frequency range. This lack of studies focused on blade elasticity is not the result of current models adequately predicting control response, as many investigators describe lingering problems, the physical origins of which are unknown or unproved, as discussed by Curtiss [8].

While the overwhelming majority of flight dynamics studies [e.g. 6, 7, 9 through 12] have relied on a rigid blade formulation of the rotor motion, with simple corrections to account for any suspected flexibility effects, some recent efforts have addressed directly the inclusion of more detailed elastic blade descriptions in flight dynamics models. Lewis [13] used the FLIGHTLAB program to simulate the control response of the UH-60 in hover and forward flight. Results were obtained using rigid and elastic blade models, in both the time and frequency domain. Although the results were somewhat inconclusive, the effects of flexibility overall seemed to be small, increasing slightly with forward speed. Turnour and Celi [14] combined a well documented aeroelastic rotor analysis code with the UM-GENHEL flight dynamics code to study the effects of blade flexibility on dynamic response. They examined the UH-60 in hover only. In this study, comparisons of rigid and elastic blade models were based on *numerically* linearized equations of motion, which necessarily restricted the conclusions to the particular helicopter and flight condition being investigated. Therefore, while [14] concludes that blade flexibility does not seem to be important for the Blackhawk in hover, extrapolation of this conclusion to other helicopters or flight conditions is not justified. Indeed, the claim, based on numerical results for the UH-60 alone, that blade flexibility has a "very small effect" on the dynamics of (all) articulated rotor helicopters in hover is shown below to be false in certain well defined circumstances.

Motivated by the above discussion, the present work has the following objectives:

- 1.) Develop an *analytical* (non-numerical) flight dynamics modelling technique which includes blade elasticity and rotor-body coupling, but is sufficiently simple to provide physical insight.
- 2.) Apply the model to selected flight dynamics problems in which blade flexibility is suspected to play a role, but which are at present not well understood. Establish the fundamental mechanisms,

if any, by which blade flexibility influences the vehicle control response in these problems.

- 3.) Evaluate the possibility of adapting rigid blade models, through the adjustment of blade root springs and dampers or other empirical model parameter adjustments, for the accurate prediction of the observed flexibility effects.

The present work does not consider the representation of hingeless rotors using an equivalent hinge offset and hinge spring. The generation of hub moments due to flapping of hingeless rotors is well understood as a result of considerable research. Thus, although the methods described below are applicable to hingeless rotors, attention is focused on the potential shortcomings of rigid blade models for representing articulated rotors. Two specific problems will be examined in detail: (i) the effects of flapping flexibility on the vertical acceleration response to collective inputs in hover; and (ii) the direct impact of a powerful lag damper on the inplane elastic blade motion and the resulting effects on the lateral and directional control responses in hover.

Description of Model

This section describes the development of the equations of motion for the coupled fuselage - flexible rotor system. More details are available in [15].

Equations for Blade Motion Derivation of the analytical dynamic model begins with consideration of the partial differential equations which govern the motion of a flexible blade. The equations use the elastic terms given by Houbolt and Brooks [16], but the loadings have been rederived, as described below. While several simplifying assumptions have been made to facilitate interpretation of the resulting equations, none of these assumptions is necessary for the subsequently described solution scheme. The chordwise locations of the elastic, neutral and mass axes of the blade are assumed to be coincident at the quarter-chord. Torsional deflections and coupling of the flap and lag motions due to blade twist have been neglected. The undeflected (straight) elastic axis is rotated about the hinge through trim flap and lag angles. The elastic deflections are relative to this initial position, which is determined as part of the trim calculations. Placing the undeflected elastic axis out of the nominal rotor plane allows the axial deflection equation to be discarded without loss of the Coriolis terms which couple flap and lag[†]. This is

[†]An alternative method for discarding the axial deflection equation while retaining important coupling terms is described by Ormiston and Hodges [5].

particularly important to the present study because the flexible blade model may be reduced to the case of rigid blades, as described below, and comparisons of the resulting equations with a previous analytical model based on rigid blades and Lagrangian dynamics [9] provide important verification of the new model.

Explicit expressions for the inertial, gravitational, and aerodynamic loadings on the blade are derived by computer symbolic manipulation (Mathematica). The position and orientation of the blade element is defined by several relative position vectors and a sequence of rotation matrices. Most elements of these vectors and matrices are functions of time and thus become the model degrees of freedom (e.g. Euler angles for the fuselage attitude). Velocities and accelerations are derived by differentiation with respect to time in the appropriate axis system. The aerodynamic loading is derived using blade-element theory, with first harmonic inflow as described by Pitt and Peters [17]. The usual simplifying assumptions have been employed in the aerodynamic model, namely neglect of: compressibility, blade stall, reversed flow, and large inflow angles.

Reduction of the partial differential equations governing the motion of an individual blade into a system of ordinary differential equations for the rotor system is described in a later section.

Equations for Body Motion The fuselage is assumed to be a rigid body undergoing arbitrary translation and rotation. The force of each blade, which acts on the fuselage at the hinge point, is calculated by integrating the blade loadings from the hinge to the blade tip. The resultant forces are resolved into fuselage (shaft-referenced) axes. Each blade also may exert root moments due to the presence of a hinge spring and/or a damper.

Other forces acting on the fuselage are gravity, which acts through the c.g. of the fuselage, and the tail rotor force. The tail rotor does not add additional dynamic states to the model, as it is described by simple analytical expressions for thrust coefficient as a function of tail rotor collective and tail rotor hub velocity. No fuselage aerodynamic forces are included for the hovering case.

Linearization of Equations Considerable research has examined the importance of retaining nonlinear terms due to "moderate blade deflections" for accurate stability calculations for hingeless rotors [4]. However, because the focus of the present work is to identify the mechanisms of interaction between the fuselage and the flexible blades, and develop analytical relationships which illuminate these

mechanisms, linearization is a useful approximation. With this approximation come limitations in any qualitative conclusions about rotor stability and small errors in quantitative prediction of control response. The results will be most useful when applied to rotors which are aeromechanically well damped, as is the case for articulated rotors with significant mechanical lag dampers.

Linearization of both the blade and fuselage equations of motion is effected by Mathematica. Partial derivatives of each equation with respect to all model degrees of freedom and all of their time derivatives are computed and evaluated symbolically for an arbitrary trim condition. As discussed above, elastic displacements are relative to an elastic axis which has undergone trim flap and lag deflections. Therefore, the trim elastic displacements are taken to be zero, and the blade trim calculation requires only the determination of the initial elastic axis orientation and is therefore equivalent to a rigid blade trim calculation.

Extended Multiblade Transformation and Galerkin Method At this stage of the derivation, the flexible displacements are expanded in a set of radial functions:

$$v^{(k)}(x, t) = \sum_{j=1}^M q_j^{(k)}(t) \phi_j(x) \quad (1)$$

This expression can be thought of as replacing the infinitely many degrees of freedom in the flexible beam with M new degrees of freedom. The $\phi_j(x)$ are any complete set of functions which satisfy the time-independent boundary conditions on the flexible beam, and therefore form a basis set for the allowable displacements. In the present case, successive ϕ_j were chosen as the lowest order polynomials which satisfied the boundary conditions and were orthogonal, with the blade mass distribution as a weighting function, to the previously chosen ϕ_j . It should be noted that the ϕ_j do not represent the modes of the blade motion. Rather, linear combinations of the ϕ_j represent approximations to the modes. This distinction will be of importance to the discussion surrounding the effects of the lag damper, and for this reason the ϕ_j will be referred to as the basis functions.

The multiblade transformation converts the degrees of freedom from those describing each rotor blade to those describing the overall state of the rotor:

$$\begin{aligned}
q_j^{(k)}(t) = & \zeta_{0j} + \zeta_{1cj} \cos(\psi^{(k)}) \\
& + \zeta_{1sj} \sin(\psi^{(k)}) + \zeta_{2cj} \cos(2\psi^{(k)}) \quad (2) \\
& + \zeta_{2sj} \sin(2\psi^{(k)}) + \dots
\end{aligned}$$

An analogous expression is used for the flapping displacements.

The body equations of motion are transformed by simply substituting equations (1) and (2) for the flexible displacements. The radial dependence of the blade deflections in these equations was previously removed when the blade loads were integrated to obtain resultant forces. These integrals are evaluated using the specified basis functions. Periodic coefficients appearing in the equations are converted into sums of nonperiodic terms and higher harmonics. The latter are discarded to obtain constant coefficient equations.

The blade equations must be converted from partial differential equations into ordinary differential equations. This is accomplished using the Galerkin procedure [18]. After substituting equation (1), the blade equations are multiplied by ϕ_i and integrated from the hinge to the blade tip. Integration by parts allows the spring and damper boundary conditions to enter the equations. This operation is repeated for $i = 1, M$ resulting in a system of ordinary differential equations, to which the multiblade transformation is applied. The higher harmonics appearing in these equations are again discarded.

In the case that $M = 1$ and $\phi_1 = x$, the rigid blade description is recovered, with ζ_{01} , ζ_{1c1} , and ζ_{1s1} corresponding to the usual multiblade lag degrees of freedom retained in flight dynamics models. Thus, the rigid blade description is a subset of the present model.

It should also be noted that the transformations described above are essentially identical in concept to those described in [14]. However, in that work, the transformations, as well as the linearization, were executed numerically.

Results and Discussion

Model Validation

Three aspects of the validation of the model will be presented here: (i) comparison with existing analytical models incorporating rigid blade dynamics; (ii) comparison of predicted control response with flight test data; and (iii) comparison of shaft-fixed invacuum flexible blade modal frequencies with previous, independent calculations.

As described above, comparison of the present model with the Princeton Hover Model [9] has been especially valuable because that model was derived from the Lagrangian point of view, so that favorable comparisons provide a truly independent confirmation that the assumptions described in the preceding sections have been properly coded. The form of the Princeton Hover Model used for these comparisons is that due to Keller [19]. This comparison also has shed light on some subtle differences between the kinematics of a deflected beam described by a single basis function, and a rotating rigid beam. These differences led to the appearance of some additional small terms in the present model, which do not appear to significantly affect the predicted response. Otherwise, the agreement on a term-by-term basis was exact up to first order in the model small parameters (such as dimensionless hinge offset).

Figure 2 shows the frequency response of roll rate to lateral cyclic for the Blackhawk, as measured from flight tests [20] and predicted by the present model and the Princeton Hover Model. The agreement is excellent up to about 1 per rev, where body modes and other unmodelled dynamics become influential and the coherence of the test data is low. The small disagreement between the predictions and the data around 0.2 per rev is associated with the coupled body-flap-inflow mode and may be due to a problem with the dynamic inflow. Further investigations into this problem are under way.

Table 1 shows the frequencies of the first and second blade bending modes in both the flap and lag directions for the CH-53E, as calculated using the present analysis with the shaft fixed, and as reported previously [21]. The agreement is good, especially in predicting the first bending mode. Further validation of the flexible blade equations is an ongoing effort.

Table 1 Normalized natural frequencies of flexible blade modes without aerodynamics.

Blade Mode	Present Model	Previous Model
first lag	3.50	3.43
second lag	8.96	8.54
first flap	2.67	2.66
second flap	5.08	4.79

Vertical Acceleration Response

The first response problem to be considered is the effect of flapping flexibility on the vertical acceleration response to collective inputs in hover. Speculation about the role of blade elasticity in the prediction of this response can be traced to a conjecture by Carpenter and Fridovich [22] that blade

flexibility was responsible for an overprediction in the thrust response of a rotor to a rapid change in collective pitch. Chen and Hindson [23] postulated that the rigid blade modelling assumption resulted in a non-physical undershoot in the vertical acceleration response. They suggested reducing the blade first mass moment of inertia, $S_{b,1}$, by 11 percent as a simple empirical means of correcting the predicted response. Houston [24] found better agreement with identified stability derivatives for the vertical response of a Puma in hover when, "on average," $S_{b,1}$ was reduced by 30 percent. In none of these references is a detailed justification given for *any* genuine effect due to blade flexibility, nor is there a correlation of such an effect with a reduction in $S_{b,1}$. The fact that the suggested correction factor varies by a factor of 3 without an explicit relation to specific blade properties signals a need for a more fundamental investigation.

The present model was simplified to consider the vertical response of a hovering helicopter by retaining only the fuselage vertical velocity, the collective inflow, and the collective flapping degrees of freedom, as well as the collective control input. When only the first (rigid) collective flapping degree of freedom is retained, the equations are identical to those employed by Chen and Hindson [23], further verifying the present results. Because it does not contribute significantly to the changes brought about by flexibility, the inflow degree of freedom is not shown explicitly in the following equations, but is retained for all numerical calculations.

The coupled vertical velocity - collective rigid flapping equations, neglecting small terms in hinge offset, are

$$(m_f + Nm_b)\dot{w} + NS_{b,1}\ddot{\beta}_{o1} = -N\Omega A_0 w - N\Omega A_1 \dot{\beta}_{o1} + N\Omega^2 \Gamma_o \vartheta_o \quad (3)$$

$$S_{b,1}\dot{w} + I_{b,1}\ddot{\beta}_{o1} = \Omega A_1 w - I_{b,1}\Omega^2 \beta_{o1} - \Omega \Gamma_1 \dot{\beta}_{o1} + \Omega^2 \Gamma_1 \vartheta_o \quad (4)$$

When the equations are written in this form, the physical nature of each term is more easily identified than when the equations are written in the first-order form

$$\dot{\underline{x}} = [A]\underline{x} + [B]u \quad (5)$$

In equations (3) and (4), each term may be identified as resulting uniquely from either aerodynamic or inertial loadings (e.g. terms on the left hand side of the equations are entirely inertial).

The short time step response of acceleration to collective pitch predicted by the model for the UH-60 Blackhawk is shown in Figure 3 and is representative of the response observed for a variety of single rotor helicopters. The rigid blade model response at $t=0^+$ shows an undershoot whose magnitude is about 10 percent of the maximum response. This undershoot is indicative of a non-minimum phase transfer function whose numerator is the same order as its denominator. Elimination of this initial undershoot was achieved by Chen and Hindson by their suggested adjustment of $S_{b,1}$. The physical reason for this undershoot can be seen by considering equations (3) and (4) at high frequencies. After taking the Laplace Transforms, and taking the limit of large s , we obtain

$$(m_f + Nm_b)sw + NS_{b,1}s^2\beta_{o1} = N\Omega^2\Gamma_o\vartheta_o \quad (6)$$

$$S_{b,1}sw + I_{b,1}s^2\beta_{o1} = \Omega^2\Gamma_1\vartheta_o \quad (7)$$

Using the second expression to eliminate the flapping acceleration from the first expression gives

$$\left(m_f + Nm_b - \frac{NS_{b,1}^2}{I_b} \right) sw = - \left[\frac{\Gamma_1}{\Gamma_o} - \frac{I_{b,1}}{S_{b,1}} \right] N\Omega^2 \frac{\Gamma_o S_{b,1}}{I_{b,1}} \vartheta_o \quad (8)$$

The expression in brackets on the right hand side of this equation is the distance between the effective point of application of the aerodynamic force due to blade pitch and the center of percussion (c.p.) of the rigid blade. For a uniform blade, this quantity is positive, as the c.p. lies at $2R/3$, while the aerodynamic force is at $3R/4$. The question to be answered is whether or not a flexible blade should be expected to have an effective center of percussion at the point of action of the aerodynamic force on the blade.

The additional (flexible) flapping degrees of freedom appear in the equations of motion in much the same way as the rigid flapping. In particular, there are terms on the right hand sides of equations (3) and (4) proportional to $\dot{\beta}_{o2}$ due to aerodynamics, and terms of the left hand sides of equation (3) proportional to $\ddot{\beta}_{o2}$, due to the acceleration of the blade center of mass. This acceleration term does not appear in the rigid flapping equation because of the selection of basis functions which are orthogonal with respect to the blade mass distribution. The $\ddot{\beta}_{o2}$

equation has exactly the same form as the rigid flapping equation. If we again consider the limit of high-frequency, we obtain the following three relations

$$(m_f + Nm_b)sw + Ns^2(S_{b,1}\beta_{o1} + S_{b,2}\beta_{o2}) = N\Omega^2\Gamma_0\vartheta_o \quad (9)$$

$$S_{b,1}sw + I_{b,1}s^2\beta_{o1} = \Omega^2\Gamma_1\vartheta_o \quad (10)$$

$$S_{b,2}sw + I_{b,2}s^2\beta_{o2} = \Omega^2\Gamma_2\vartheta_o \quad (11)$$

where $S_{b,2}$ represents the blade c.m. displacement due to the second degree of freedom and Γ_2 is a result of the fact that the second flap basis function is not orthogonal to the aerodynamic loading distribution which results from collective pitch. The magnitude of Γ_2 is a measure of the extent to which the second degree of freedom is affected by the aerodynamic loading. As before, these equations may be combined to eliminate the flapping degrees of freedom:

$$\left(m_f + Nm_b - \frac{NS_{b,1}^2}{I_{b,1}} - \frac{NS_{b,2}^2}{I_{b,2}} \right) sw = - \left[\frac{\Gamma_1}{\Gamma_0} - \frac{I_{b,1}}{S_{b,1}} \left(1 - \frac{S_{b,2}\Gamma_2}{I_{b,2}\Gamma_1} \right) \right] N\Omega^2 \frac{S_{b,1}\Gamma_0}{I_{b,1}} \vartheta_o \quad (12)$$

Comparison with equation (8) reveals that flexibility alters the effective location of the blade c.p. Depending on the signs of $S_{b,2}$ and Γ_2 , this change may move the c.p. closer to or further from the point of application of the aerodynamic force. The value of Γ_2 reflects the influence of aerodynamic loading on the second flap basis function, and will depend on the basis shape, but is generally small and positive. The value of $S_{b,2}$ indicates the magnitude of displacement of the blade c.m. due to the second basis, and depends on the basis shape and also on the blade mass distribution. Note that the c.p. location would be further affected by inclusion of additional basis functions, but that these effects diminish quite rapidly, as the c.m. displacements and aerodynamic forcings of these higher functions are quite small.

The general conclusion to be drawn from the preceding analysis is that, while flapping flexibility does in fact have an impact on the initial acceleration response, it is by no means certain that this effect will always reduce the predicted undershoot, and there is, in general, no reason to expect the undershoot to vanish *because of blade flexibility*. It is more likely that the lack of initial undershoot in the experimental

vertical acceleration response is due to a non-ideal step input (i.e. an initial ramp) in the test data, as shown in Figure 4, where the current model is compared to flight data for the UH-60 in hover. It is clear that when the model is forced by the actual collective input, there is no initial undershoot. The small difference between the data and the model is not corrected by inclusion of blade flexibility. Indeed, for the range of frequencies excited by the actual input, the rigid and flexible models predict nearly identical acceleration responses.

The consequences of empirical adjustments to $S_{b,1}$ on the acceleration transfer function, when using a carefully derived model, are relatively minor, appearing only at frequencies near the rotor speed and higher. (That the low frequency residualized dynamics are independent of blade mass distribution was noted by Chen and Hindson.) However, two drawbacks of such modifications should be heeded. First, there is the risk of conveying to the control system designer an over-confidence in the valid bandwidth of the model. Second, such modifications encourage further extrapolations of the notion that flexibility results in "overprediction of blade inertial forces" on the hub. These extrapolations are unfounded and potentially create significant, but erroneous, changes in the predictions of the response of other degrees of freedom.

Lag Dampers and Flexibility

Hong and Curtiss [25] and Curtiss [8] have shown that the presence of a powerful lag damper, such as that used on the CH-53E, modifies the blade boundary condition in a way that causes the first lag mode to be poorly predicted by the traditional hinged, rigid blade approximation. The damper was shown to convert the lowest mode into a sort of "hybrid" between the hinged and cantilever mode shapes. For weak dampers, the mode is very nearly the same as the hinged mode, while for very powerful dampers, the mode becomes entirely cantilever. The changes in the eigenvalue of the lag mode, calculated for an isolated rotor, were shown to be consistent with discrepancies between the flight-test data and predictions of the roll rate response to lateral cyclic. In what follows, these prior results are expanded and clarified, and simplified equations which explicitly describe the coupled body - flexible rotor dynamics are presented.

Before considering the body - rotor coupling, it is useful to examine the effects on the inplane motion of the damper induced flexibility. In the interest of simplicity, the following uncoupled equation for the inplane motion of a single blade will be used:

$$(EIv'')'' - (Tv')' + m\ddot{v} = p \quad (13)$$

where p represents the loading, which may be due to aerodynamics, Coriolis (flap coupling) forces, etc. The boundary conditions for this equation are

$$\begin{aligned} v(0,t) &= 0 \\ EIv''(0,t) &= D\dot{v}'(0,t) \\ EIv''(L,t) &= 0 \\ [EIv'''](L,t) &= 0 \end{aligned} \quad (14)$$

The second boundary condition represents the effects of the root damper. Using the Galerkin procedure described above, equation (13) was converted to a system of ordinary differential equations, which describe the time-history of the chosen basis functions. Forcing terms appear in these differential equations as representations of the loading.

In the absence of loading, $p = 0$, equation (13) with the boundary conditions (14) is an eigenvalue problem. The resulting eigenvalues may be compared to the rigid blade lag eigenvalues as a measure of the effects of blade flexibility. Figure 5 shows a comparison of the variation of the eigenvalues of rigid and flexible rotating blades as the damper magnitude is increased (after Curtiss [8]). As the damper becomes very large, the rigid blade analysis predicts two modes--one highly damped mode corresponding to a rapid decay of any initial velocity; and one lightly damped mode corresponding to a very slow return of the blade to the equilibrium condition, with the spring and damper forces playing the dominant roles. When flexibility is considered, we expect to find a limit on the faster mode. That is, for very large damping *at the root*, an initial velocity would not decay quickly, but would excite the flexible displacements. Thus, the faster rigid mode is not physically correct for sufficiently powerful dampers. On the other hand, the slower real mode persists even with flexible blades, because an initial displacement will in fact slowly be drawn back to the equilibrium position. This slower mode is seen in Figure 5 along the negative real axis. For blade parameters representative of the CH-53E, this "extra" mode is in the frequency domain of interest to flight dynamics.

An approximate method to quantify the effects on different helicopters of inplane flexibility associated with the lag damper is to compute the percent difference, Δ , between the rigid blade eigenvalue and the flexible blade first oscillatory eigenvalue. With uniform mass and stiffness distributions, three dimensionless parameters are important to the determination of this error:

$$\Delta = F\left(\frac{e}{L}, \frac{D}{m\Omega L^3}, \frac{EI}{m\Omega^2 L^4}\right) \quad (15)$$

The dependence of the error on the dimensionless damper and stiffness (hinge offset has a small effect on the *percent* error) is shown in Figure 6 as a contour plot. The values corresponding to the UH-60 and the CH-53E are plotted in the figure.

From Figure 6, we may conclude that the UH-60 should be relatively unaffected by lag damper induced flexibility. This is consistent with a more detailed study of the UH-60 in hover [14]. However, the change in the first lag mode eigenvalue of the CH-53E as a result of blade flexibility warrants a closer look, and all subsequent discussions will be directed toward this helicopter.

For both of the control response problems considered below, it will be argued that the primary coupling of the lag to the body is through the lag inertial terms, as the aerodynamic terms resulting from lag motion are small. In the rotating frame, the inertial terms may be examined by considering the motion of the center of mass of a blade, which is given by a linear combination the degrees of freedom:

$$v_{cm}(t) = \sum_{j=1}^M S_{b,j} q_j(t) \quad (16)$$

Figure 7 shows the frequency response of v_{cm} to a linear distribution of loading, which is representative of Coriolis or aerodynamic forcing. Also shown in figure 7 is the response of the c.m. displacement due to the first basis function only ($v_{cm} = S_{b,1} q_1$), computed using the same total number of basis functions. It is clear from the figure that the higher basis functions contribute only a very small amount to the total c.m. displacement response. This is because the shape of the first damper mode is almost identical to the first basis function, which is simply the rigid deflection. The primary effect of the damper-induced flexibility is a modification of the *eigenvalue* of the mode, with relatively minor changes to the *eigenfunction* (mode shape).

Based on this conclusion, one might think it possible to accurately represent the response of the c.m. of the blade using a rigid blade model with non-physical values of hinge spring and damper to match the flexible blade eigenvalue. The predicted response from such a model, with the spring and damper chosen to exactly match the oscillatory first lag mode, is also shown in Figure 7. There is considerable disagreement in the magnitude of the

calculated responses at low frequency, due to the large root spring. The reason for the phase disagreement at frequencies near the lag mode is the presence of the "extra" lag mode described above. In the transfer function of c.m. displacement to applied loading, the "extra" mode creates a pole-zero pair which lies on the real axis. This pole-zero pair makes it impossible for a simple rigid blade model to match the flexible blade model, despite the ability to match the oscillating eigenvalue exactly. Note that when the multiblade transformation is applied to examine the effects of the lag motion on the cyclic variables (e.g. pitch rate), the extra mode will be oscillatory at 1 per rev, and thus will not have as important an impact as it will have on the collective degrees of freedom.

Yaw Response to Pedal In this section, the yaw acceleration response to pedal inputs is considered in the frequency range of 0.1 to 1.0 per rev. In this frequency range, the coupling of the yaw response to the vertical velocity, collective inflow and flapping is weak, allowing only the yaw and the collective lag to be retained. The yaw equation which results from the derivation described above includes all of the forces and moments transmitted at the hinge. Combination of this equation with the collective lag equation yields the simpler equation which describes the total angular momentum of the entire vehicle about the shaft axis:

$$I_2 \ddot{r} + N I_{b,1} \ddot{\zeta}_{01} + e(S_{b,1} \ddot{\zeta}_{01} + S_{b,2} \ddot{\zeta}_{02} + \dots) = N_r r + (\text{lag aero terms}) + N_{\delta_p} \delta_p \quad (17)$$

Terms on the left-hand side of this equation represent the rate of change of total angular momentum, while terms on the right represent external torques. Note that, with the equation in this form, the lag damper and spring terms do not appear. The yaw damping, N_r/I_2 , is due to a combination of rotor aerodynamics and tail rotor force, and is small. Similarly, the lag aerodynamic terms are small in the frequency range of interest. The lag inertial terms express the change in angular momentum of the rigid mode plus the angular momentum due to the acceleration of the c.m. of the blade. In the frequency range of interest, the yaw equation states that yaw acceleration is forced by pedal inputs and acceleration of the lag degrees of freedom.

The equation for the first lag basis function degree of freedom is

$$\begin{aligned} & -(I_{b,1} + e S_{b,1}) \ddot{r} + I_{b,1} \ddot{\zeta}_{01} = \\ & -e \Omega^2 (S_{b,1} \zeta_{01} + S_{b,2} \zeta_{02} + \dots) \\ & - D(\sigma_1 \dot{\zeta}_{01} + \sigma_2 \dot{\zeta}_{02} + \dots) \\ & + (\text{small aero terms}) \end{aligned} \quad (18)$$

where σ_j is the slope of the j -th basis function at the root and "small aero terms" includes lag and yaw aerodynamics. The equations for the higher basis functions have the same form, with additional spring terms due to flexibility. Neglecting the small aerodynamic terms, these equations are just the modal expansions of the shaft-fixed lag equations considered previously, with the yaw acceleration as a uniform applied loading.

The frequency response of the yaw acceleration to pedal input is shown in Figure 8. Also shown in this figure is the response calculated using the rigid blade model, with the actual damper value and with the eigenvalue-matching spring and damper. The error in the lag eigenvalue for the basic rigid blade model is apparent. For the rigid blade model with the "adjusted" root constraints, the differences between the two predictions are a result of the "extra" real lag mode, as described above. The flexible lag modes introduce three pole-zero pairs in the transfer function between 0.2 and 0.8 per rev, which cannot be duplicated by the rigid blade model.

Although the yaw acceleration response has provided a simple and clear example of the impact of damper induced flexibility, it should be noted that these effects are relatively small in the present case because the fuselage inertia of the CH-53E is large compared to the inertia of the rotor. The effects could have some importance in the design of a high bandwidth flight control system to command yaw attitude.

Roll Response to Lateral Cyclic The coupling of the rigid lag degrees of freedom to the roll rate was shown by McKillip and Curtiss [26] and Curtiss [27] to be due primarily to the inertial terms, as the aerodynamic terms due to lag motion are small. The approximate expression for the roll moment due to lag motion, given in terms of the present notation, is:

$$\text{Roll Moment} = \frac{Nh}{2} S_{b,1} \ddot{\zeta}_{1c1} \quad (19)$$

The dominant lag terms in the roll rate equation in the case of flexible blades is found from the present analysis to take the following form:

$$\frac{Nh}{2} (S_{b,1} \ddot{\zeta}_{1c1} + S_{b,2} \ddot{\zeta}_{1c2} + \dots) \quad (20)$$

Thus, the coupling in the flexible blade case is also described by the inplane acceleration of the blade center of mass.

Figure 9 compares the frequency response of roll rate to lateral cyclic for the same three models used in figure 8. The first model shown in the figure is the present analysis which properly accounts for the effects of blade flexibility. The second model is the rigid blade model with the physically correct damper value and no spring. The changes introduced by flexibility are smaller than would be expected in light of the dramatic change in the lag eigenvalue. The reason for this is that the lag motion shows up in the transfer function as a pole-zero pair. For the CH-53E, the zero is closer to the imaginary axis, and thus dominates the frequency response curve. This zero seems to be relatively less affected by the flexibility than the lag pole. However, the change is in the direction indicated by the data [8]. The final curve in figure 9 is a rigid blade model with the eigenvalue-matching spring and damper constants. This model shows significant disagreement with both of the other models, and is therefore not an adequate representation. More appropriate methods of modifying a rigid blade model to obtain a reasonable approximation of flexibility effects are under investigation.

Conclusions

This paper described a novel technique for the development of analytical (non-numerical) equations for the coupled dynamics of the fuselage and the flexible rotor blades. A modal expansion in the radial direction and a multiblade transformation to eliminate the azimuthal harmonics were combined to produce a simplified model which was applied to three control response problems:

1.) Flapping flexibility was shown to have a small impact on the initial response of vertical acceleration to collective inputs. This effect was explained by calculation of an effective center of percussion for the flexible blade. The sign of the effect depended on the distribution of mass in the blade, and one should not generally expect the effect to reduce the initial undershoot predicted by rigid blade models. Alteration of the blade first mass moment of inertia to account for this effect is possible, but not recommended, as it conveys a false sense of confidence in the useful bandwidth of the model.

2.) Damper induced inplane flexibility was shown to modify the coupling of the yaw acceleration to the lag motion. In particular, the presence of an "extra" mode due to the flexible blade creates a pole-zero pair in the transfer function of yaw acceleration to pedal input. This effect cannot be approximated using an equivalent rigid blade model.

3.) The previously observed importance of inplane flexibility for the prediction of roll rate response to lateral cyclic was confirmed. The coupling was shown to be analogous to the rigid blade case in that it depends primarily on the lateral acceleration of the rotor center of mass. The effect of blade flexibility on the frequency response function is less dramatic than might be expected based on the changes in the first lag mode eigenvalue, because the frequency response depends also on the location of the lag-mode zero in the transfer function. The rigid blade model with nonphysical spring and damper values was not adequate for approximating the changes caused by lag flexibility.

Future work will extend the present results to forward flight, where previous research has indicated that aerodynamics heighten the importance of the shape of the blade modes. The fundamental effects of torsion and flap-lag flexible coupling on control response are also problems for which the present methodology is well-suited.

Acknowledgments

This work was supported by NASA Ames, Grant 2-561.

Nomenclature

$[A]$	generic system matrix, Eqn. 5
a	blade lift curve slope
$[B]$	generic control matrix, Eqn. 5
c	blade chord
D	lag damper strength
EI	blade bending stiffness
e	hinge offset
F	function describing difference between rigid and flexible blade eigenvalues
$I_{b,j}$	blade second mass integral for j -th basis function, $I_{b,j} = \int_0^L m \phi_j^2 dx$
I_z	total yaw inertia of fuselage and rotor
L	blade length, $R-e$
M	number of basis functions in expansion of flexible displacements
m	blade mass per unit length
m_b	blade mass
m_f	fuselage mass
N	number of blades
N_r	yaw moment due to yaw rate
N_{δ_p}	yaw moment due to pedal input
p	blade loading, Eqn. 13

q_j	amplitude of j -th basis function in solution of uncoupled inplane bending
R	rotor radius
r	fuselage yaw rate
$S_{b,j}$	blade first mass integral for j -th basis function, $S_{b,j} = \int_0^L m\phi_j dx$
s	Laplace transform variable
T	axial blade tension, $T(x) = \Omega^2 \int_x^L m(\xi + e) d\xi$
t	time
\underline{u}	generic control input, Eqn. 5
v	inplane flexible displacement
v_{cm}	displacement of center of mass of flexible blade
w	fuselage vertical velocity, positive up
x	radial distance from hinge point
\underline{x}	generic state vector, Eqn. 5
β_{0j}	collective, j -th basis function flap degree of freedom
Γ_j	second aerodynamic integral, $\Gamma_j = \rho ac \int_0^L (x+e)^2 \phi_j dx$
γ	Lock number, $\gamma = \frac{\rho ac R^4}{I_{b,1}}$
Δ	percent difference between the rigid and flexible eigenvalues of the rotating beam, $\Delta = \frac{ \lambda_{flex} - \lambda_{rigid} }{ \lambda_{rigid} }$
δ_p	tail-rotor pedal input
ζ_{0j}	collective, j -th basis function lag degree of freedom
ζ_{ncj}	n -th cosine harmonic, j -th basis function lag degree of freedom
ζ_{nsj}	n -th sine harmonic, j -th basis function lag degree of freedom
ϑ_o	collective pitch input
Λ_j	first aerodynamic integral, $\Lambda_j = \rho ac \int_0^L (x+e)\phi_j dx$
λ	isolated rotor blade eigenvalue
ρ	air density
σ_j	slope of j -th basis function at the hinge, $\sigma_j = \phi_j'(0)$

ϕ_j	j -th basis function
ψ	blade azimuth angle
Ω	rotor speed
$()^{(k)}$	k -th blade
$()'$	spatial derivative, $\frac{\partial}{\partial x}$
$(\dot{\quad})$	time derivative, $\frac{\partial}{\partial t}$

Notes:

- 1.) Γ_0 and Λ_0 are computed with $\phi_0 = 1$.
- 2.) For hinged blades, neglecting small terms in hinge offset, the following equivalencies apply: $\Gamma_0 = \frac{\gamma_b}{6R}$, $\Gamma_1 = \frac{\gamma_b}{8}$, $\Lambda_0 = \frac{\gamma_b}{4R^2}$,
 $\Lambda_1 = \frac{\gamma_b}{6R}$

References

1. Blake, B.B., and I.B. Alansky, "Stability and Control of the YUH-61A", *Journal of the American Helicopter Society*, Vol. 22, No. 1, January 1977..
2. Celi, R., "Effect of Hingeless Rotor Aeroelasticity on Helicopter Longitudinal Flight Dynamics", *Journal of the American Helicopter Society*, Vol. 36, No. 1, January 1991.
3. Chopra, I., "Perspectives in Aeromechanical Stability of Helicopter Rotors", *Vertica*, Vol. 14, No. 4, 1990.
4. Friedmann, P.P., "Helicopter Rotor Dynamics and Aeroelasticity: Some Key Ideas and Insights", *Vertica*, Vol. 14, No. 1, 1990.
5. Ormiston, R.A., and D.H. Hodges, "Linear Flap-Lag Dynamics of Hingeless Rotor Blades in Hover", *Journal of the American Helicopter Society*, Vol. 16, No. 2, April 1972.
6. Curtiss, H.C., Jr., "Stability and Control Modelling", *Vertica*, Vol. 12, No. 4, 1988, pp. 381-394.
7. Chen, R.T.N., and W.S. Hindson, "Influence of High-Order Dynamics on Helicopter Flight-Control System Bandwidth", *Journal of Guidance, Control, and Dynamics*, Vol. 9, No. 2, 1986, pp. 190-197.

8. Curtiss, H.C., Jr., "On the Calculation of the Response of Helicopters to Control Inputs", *18th European Rotorcraft Forum*, Avignon, France, September 1992.
9. Zhao, X., and H.C. Curtiss, Jr., "A Linearized Model of Helicopter Dynamics Including Correlation with Flight Test", *2nd International Conference on Rotorcraft Basic Research*, College Park, MD, February 1988.
10. Kim, F.D., R. Celi, and M.B. Tischler, "Formulation and Validation of High-Order Linearized Models of Helicopter Flight Mechanics", *46th AHS Annual Forum*, Washington, DC, May 1990.
11. Ballin, M.G., and M.-A. Dalang-Secréstan, "Validation of the Dynamic Response of a Blade-Element UH-60 Simulation Model in Hovering Flight", *Journal of the American Helicopter Society*, Vol. 36, No. 4, October 1991, pp. 77-88.
12. Chaimovich, M. et al., "Investigation of the Flight Mechanics Simulation of a Hovering Helicopter", *48th AHS Annual Forum*, Washington, DC, June 1992.
13. Lewis, W.D., "An Aeroelastic Model Structure Investigation for a Manned Real-Time Rotorcraft Simulation", *49th AHS Annual Forum*, St. Louis, MO, May 1993.
14. Turnour, S.R., and R. Celi, "Effects of Blade Flexibility on Helicopter Stability and Frequency Response", *19th European Rotorcraft Forum*, Cernobbio, Italy, September 1993.
15. Kothmann, B.D., "Development of an Analytical Helicopter Dynamics Model Including Flexible Blades", MAE Department Report in Preparation, Princeton University, 1995.
16. Houbolt, J.C., and Brooks, G.W., "Differential Equations of Motion for Combined Flapwise Bending, Chordwise Bending, and Torsion of Twisted Nonuniform Rotor Blades", NACA Report 1346, Langley Field, VA, 1958.
17. Pitt, D.M., and D.A. Peters, "Theoretical Prediction of Dynamic Inflow Derivatives", *Vertica*, Vol. 5, 1981, pp. 21-34.
18. Finlayson, B.A., *The Method of Weighted Residuals and Variational Principles*, Academic Press, New York, 1972.
19. Keller, J.D., "Analytical Linear Equations for the Lateral-Longitudinal Dynamics of a Single Rotor Helicopter, Retaining Terms up to First Order", Unpublished Notes, 1993.
20. Fletcher, J.W., "Identification of UH-60 Stability Derivative Models in Hover from Flight Test Data", *49th AHS Annual Forum*, St. Louis, MO, May 1993.
21. Hong, S.W., "An Analytic Modeling And System Identification Study of Helicopter Dynamics", PhD Dissertation, Yale University, May 1993.
22. Carpenter, P.J., and B. Fridovich, "Effect of a Rapid Blade-Pitch Increase on the Thrust and Induced-Velocity Response of a Full-Scale Helicopter Rotor", NACA Technical Note 3044, Washington, DC, November 1953.
23. Chen, R.T.N., and W.S. Hindson, "Influence of Dynamic Inflow on the Helicopter Vertical Response", *Vertica*, Vol. 11, No. 1/2, 1987, pp. 77-91.
24. Houston, S.S., "Identification of a Coupled Body/Coning/Inflow Model of Puma Vertical Response in Hover", *Vertica*, Vol. 13, No. 3, 1989, pp. 229-249.
25. Hong, S.W., and H.C. Curtiss, Jr., "An Analytic Modeling And System Identification Study of Rotor/Fuselage Dynamics At Hover", *Mathematical and Computer Modelling*, Vol. 19, No. 3/4, February 1994, pp. 47-67.
26. McKillip, R., Jr., and H.C. Curtiss, Jr., "Approximations for Inclusion of Rotor Lag Dynamics in Helicopter Flight Dynamics Models", *17th European Rotorcraft Forum*, Berlin, Germany, September 1991.
27. Curtiss, H.C., Jr., "Physical Aspects of Rotor Body Coupling in Stability and Control", *46th AHS Annual Forum*, Washington, DC, May 1990.

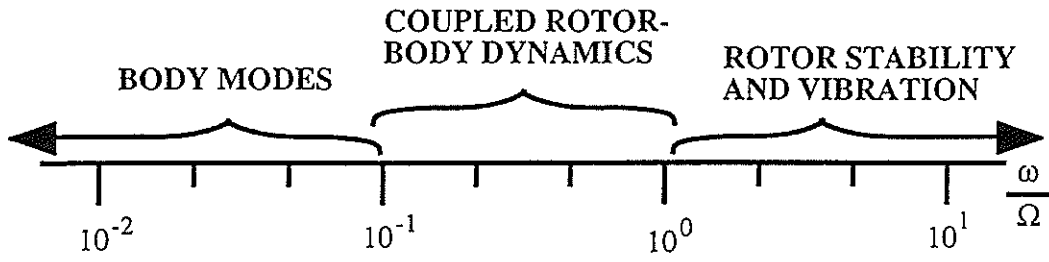


Figure 1. Approximate regions of validity for various types of flexible blade analyses.

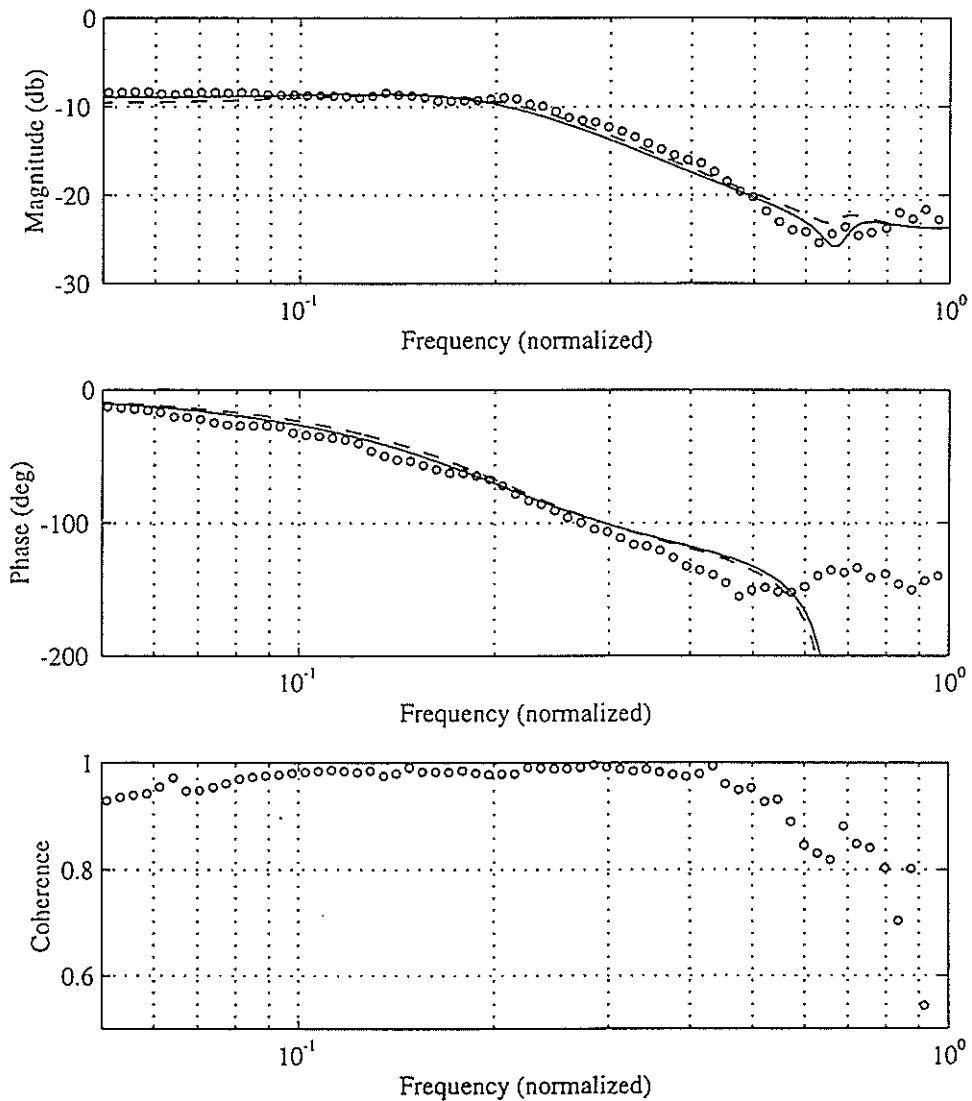


Figure 2. Frequency response of roll rate to lateral cyclic stick for the UH-60 in hover. Solid line = present model, dashed line = Princeton Hover Model, o = flight test data.

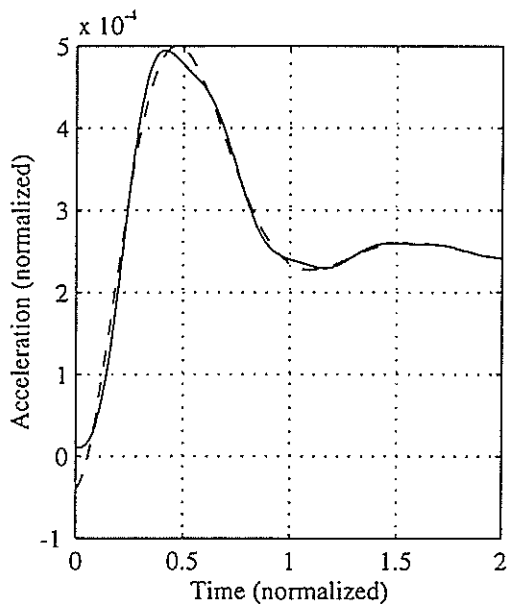


Figure 3. Time response of vertical acceleration to collective stick ideal step input. Solid line = flexible blade analysis, dashed line = rigid blade analysis. (Acceleration normalized by $\Omega^2 L$; time normalized by Ω^{-1})

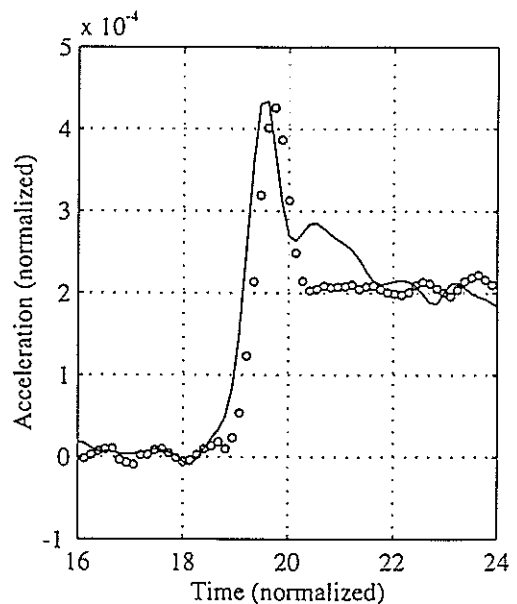


Figure 4. Time response of vertical acceleration to collective stick nonideal step input, for UH-60 in hover. Solid line = flexible blade model, dashed line = rigid blade model, o = flight test data. (Flexible and rigid models predict nearly identical response.)

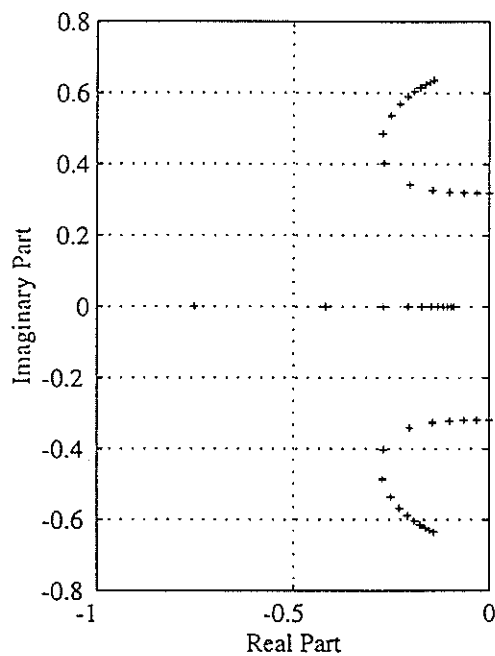
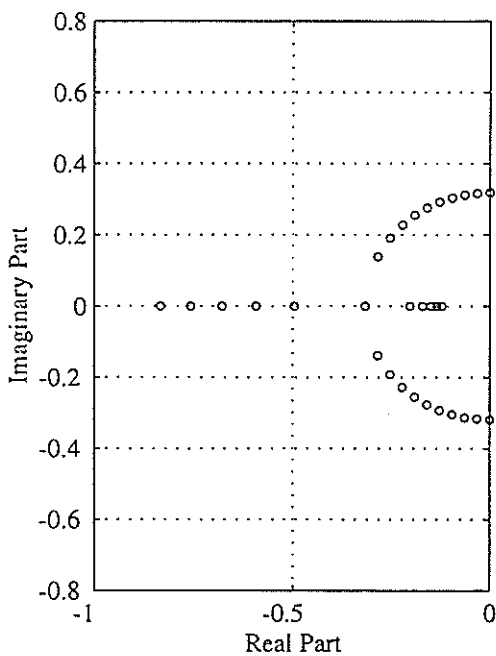


Figure 5. Variation of normalized eigenvalues of inplane motion of rotating blade with damper constant. Points shown correspond to a rigid blade damping ratio varying from 0.0 to 1.5, in steps of 0.1. Mass and stiffness distributions represent a CH-53E blade. o=rigid blade, +=flexible blade.

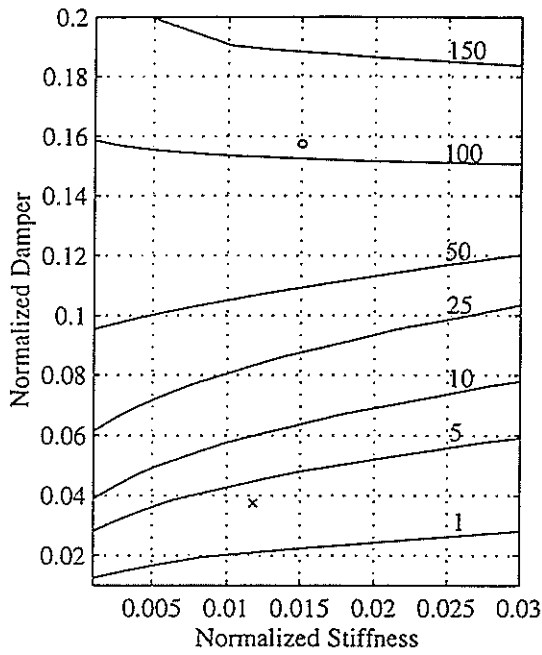


Figure 6. Contours of constant percentage difference, Δ , in rotating beam first eigenvalue between flexible and rigid blade analyses. \circ =CH-53E, \times =UH-60. Numbers indicate percentages.

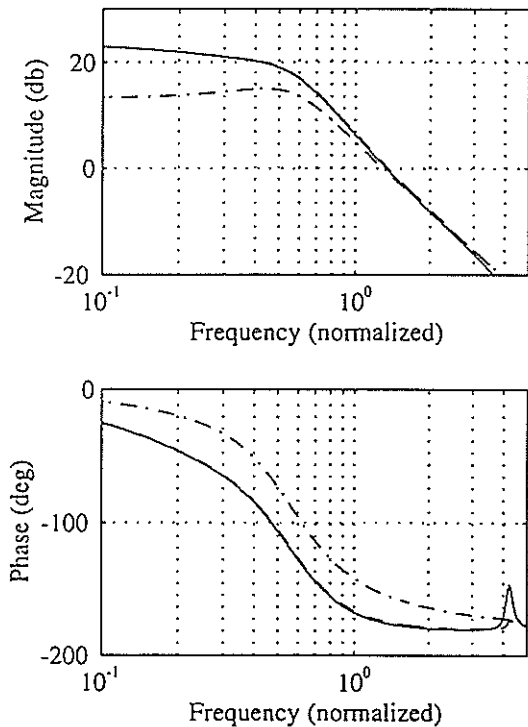


Figure 7. Frequency response of blade c.m., v_{cm} , to linear loading distribution. Solid line = flexible blade analysis, dashed line = flexible blade analysis with approximate c.m. location, dot-dashed line = "equivalent" rigid blade analysis.

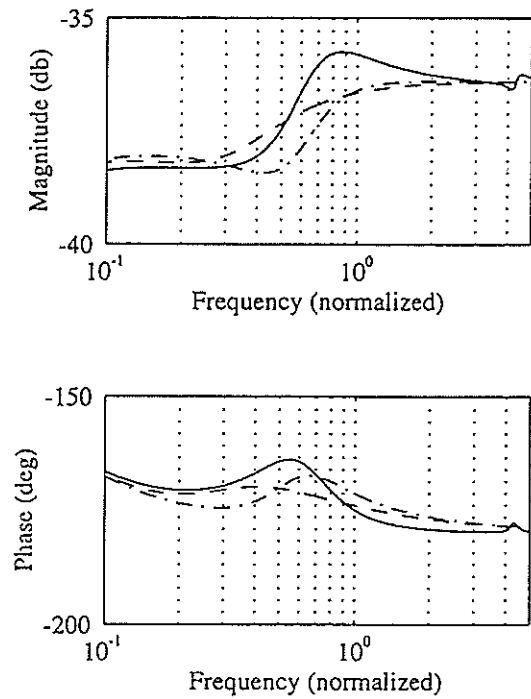


Figure 8. Frequency response of yaw acceleration to tail rotor collective pitch for CH-53E in hover. Solid line = flexible blade analysis, dashed line = rigid blade analysis, dot-dashed line = "equivalent" rigid blade analysis.

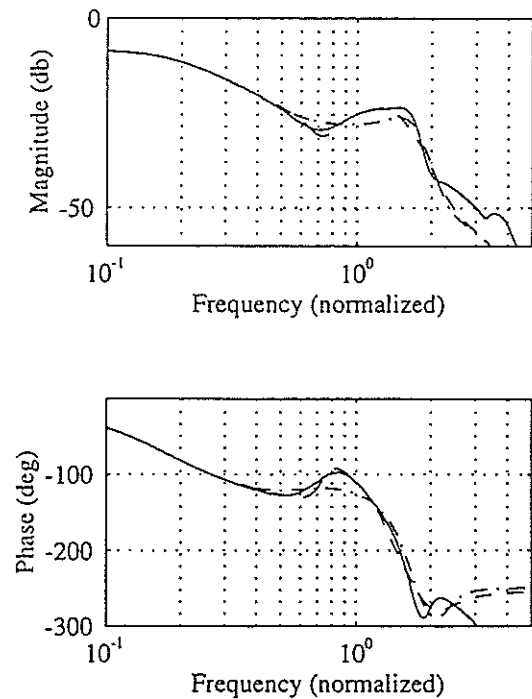


Figure 9. Frequency response of roll rate to lateral cyclic input for the CH-53E in hover. Lines as in Figure 8.